International Journal of Pharmaceutics 657 (2024) 124131

Contents lists available at ScienceDirect

International Journal of Pharmaceutics

journal homepage: www.elsevier.com/locate/ijpharm

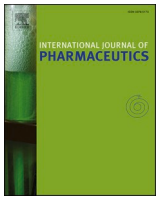

Prolonged delivery of HIV-1 vaccine nanoparticles from hydrogels

Raphael Mietzner [a], Clara Barbey [a], Heike Lehr [a], Christian E. Ziegler [a], David Peterhoff [b,c], Ralf Wagner [b,c], Achim Goepferich [a], Miriam Breunig [a,*]

[a] Department of Pharmaceutical Technology, University of Regensburg, Universitaetsstrasse 31, 93040 Regensburg, Germany
[b] Institute of Medical Microbiology and Hygiene, University of Regensburg, Universitaetsstrasse 31, 93040 Regensburg, Germany
[c] Institute of Clinical Microbiology and Hygiene, University Hospital Regensburg, Regensburg, Germany

ARTICLE INFO

Keywords:
HIV vaccine
PEG hydrogel
Sustained release
Silica nanoparticles
Env
Co-delivery
Antigen PEGylation

ABSTRACT

Immunization is a straightforward concept but remains for some pathogens like HIV-1 a challenge. Thus, new approaches towards increasing the efficacy of vaccines are required to turn the tide. There is increasing evidence that antigen exposure over several days to weeks induces a much stronger and more sustained immune response compared to traditional bolus injection, which usually leads to antigen elimination from the body within a couple of days. Therefore, we developed a poly(ethylene) glycol (PEG) hydrogel platform to investigate the principal feasibility of a sustained release of antigens to mimic natural infection kinetics. Eight-and four-armed PEG macromonomers of different MWs (10, 20, and 40 kDa) were end-group functionalized to allow for hydrogel formation via covalent cross-linking. An HIV-1 envelope (Env) antigen in its trimeric (Env_{tri}) or monomeric (Env_{mono}) form was applied. The soluble Env antigen was compared to a formulation of Env attached to silica nanoparticles (Env-SiNPs). The latter are known to have a higher immunogenicity compared to their soluble counterparts. Hydrogels were tunable regarding the rheological behavior allowing for different degradation times and release timeframes of Env-SiNPs over two to up to 50 days. Affinity measurements of the VCR01 antibody which specifically recognizes the CD4 binding site of Env, revealed that neither the integrity nor the functionality of Env_{mono}-SiNPs (K_d = 2.1 ± 0.9 nM) and Env_{tri}-SiNPs (K_d = 1.5 ± 1.3 nM), respectively, were impaired after release from the hydrogel (K_d before release: 2.1 ± 0.1 and 7.8 ± 5.3 nM, respectively). Finally, soluble Env and Env-SiNPs which are two physico-chemically distinct compounds, were co-delivered and shown to be sequentially released from one hydrogel which could be beneficial in terms of heterologous immunization or single dose vaccination. In summary, this study presents a tunable, versatile applicable, and effective delivery platform that could improve vaccination effectiveness also for other infectious diseases than HIV-1.

1. Introduction

Although immunization seems a captivating easy concept, launching an effective vaccine remains for some pathogens like HIV-1 a challenge (Palgen et al., 2021). Therefore, many concepts have been investigated for controlling response to a vaccine such as creating an inflammatory niche at the injection site (Roth et al., 2022), engineering more stable and affine antigens (Peterhoff and Wagner, 2017), or targeting specific immune cells (Roth et al., 2022). However, one promising aspect has been widely neglected – the kinetics of antigen presentation (Cirelli and Crotty, 2017b). Conventional vaccination requires multiple visits to a doctor to realize the so called prime-boost regime. A defined dose of an antigen is administered as bolus injection at fixed time intervals. Thus, a protein-based antigen is detected in draining lymph nodes within minutes to a few hours but is largely flushed away within one to two days (Cirelli and Crotty, 2017a; Moon et al., 2012). In contrast, natural infections expose the immune system to escalating antigen amounts, and inflammation may proceed over days to several weeks (Cirelli and Crotty, 2017a; Moon et al., 2012). Thus, we are far away from mimicking a natural infection kinetics when applying a conventional prime-boost vaccination regime. Recent publications addressed this issue and provided evidence that antigen exposure in draining lymph nodes over several days triggers a much stronger immune response than traditional bolus injection (Lofano et al., 2020). For example, Tam et al. exposed mice to different antigen kinetics by using repeated injections or mini-osmotic pumps and compared the results to traditional bolus immunization (Tam et al., 2016). An extended antigen dosing profile over two weeks generally improved humoral responses. In addition, a

* Corresponding author.
E-mail address: miriam.breunig@ur.de (M. Breunig).

https://doi.org/10.1016/j.ijpharm.2024.124131
Received 13 February 2024; Received in revised form 14 April 2024; Accepted 15 April 2024
Available online 21 April 2024

continuous exposure enhanced formation of germinal centers (GC), which are microanatomical structures that are an important part of the B cell humoral immune response (Victora and Nussenzweig, 2022), and higher serum antibody responses were realized (Tam et al., 2016). In this study, also two dosing profiles, each spanning a period of two weeks, were compared. The exponentially increasing dosing of an antigen was superior compared to a constant exposure regarding the duration of antigen retention in lymph nodes, and the number of B cells in GCs (Tam et al., 2016). Cirelli and co-workers applied these findings to nonhuman primates. Surgically implantable mini-osmotic pumps were used to slowly deliver an HIV-1 vaccine over a period of up to four weeks, thereby improving HIV-specific GC formation and the quality of neutralizing antibodies (Cirelli et al., 2019). However, implementation of repeated injection schedules or surgical implantable mini-osmotic pumps are impractical for global distribution of prophylactic vaccines. Therefore, more suitable vaccine delivery platforms are needed that fulfill requirements for an application especially in countries of the developing world with limited healthcare access.

Multiple materials and technologies are currently being investigated in the preclinical stage to enable programmed antigen release (Lofano et al., 2020), like e.g. implants, injectable microparticles, and microneedle patches (DeMuth et al., 2013; DeMuth et al., 2014; Liu et al., 2014; Noh et al., 2016; Slobbe et al., 2003; Thalhauser et al., 2020c). Microparticles have been shown to allow for a pulsatile release kinetics, with the antigen being released in a wavelike fashion mimicking a multibolus schedule (Guarecuco et al., 2018). Transdermal antigen delivery via microneedle patches is very attractive because it provides a way to encapsulate the antigen in a stable state prior to use and the richness of antigen-presenting cells in the intradermal region is beneficial for vaccination (Lofano et al., 2020; Menon et al., 2021). Unfortunately, these technologies still suffer from two major drawbacks: (I) Usually, they enable zero-order kinetics, in which an almost constant release of the antigen lasts for days or weeks. However, an infection-like, exponential release remains difficult to realize (Lofano et al., 2020). (II) As yet, only soluble antigens have been delivered, but not antigens immobilized on the surface of nanoparticles (NPs). The latter have been shown to increase the antigenicity of a vaccine compared to soluble antigens (Brinkkemper and Sliepen, 2019; Brouwer and Sanders, 2019; Thalhauser et al., 2020a). Microparticles and microneedle patches suffer from the limited amount of NPs that can be delivered, and may not be able to ensure particle stability or functionality (Jiang et al., 2022; Thalhauser et al., 2020c).

Hydrogels may overcome the above-mentioned shortcomings: They have been shown to release proteins with tunable release kinetics including sigmoidal, delayed, burst, or continuous release profiles from hours over several months while protecting them against degradation (Brandl et al., 2010; Gregoritza et al., 2016a; Gregoritza et al., 2017; Gregoritza et al., 2016b; Li and Mooney, 2016; Schweizer et al., 2013; Ziegler et al., 2021). Additionally, due to their cross-linked three-dimensional structure, they even allow for the incorporation and controlled release of NPs (Giovannini et al., 2017; Nunes et al., 2022). For vaccination, hydrogels have been used to co-deliver ovalbumin and an adjuvant to improve the immune response in mice (Gale et al., 2021; Roth et al., 2020). However, to the best of our knowledge, the release of an antigen covalently attached to NPs from hydrogels for vaccination has never been realized.

The goal of this study was to demonstrate the principal feasibility of a sustained release of antigen decorated NPs from hydrogels with the aim to mimic the prolonged antigen exposure of a natural infection. We developed a poly(ethylene) glycol (PEG)-based hydrogel platform comprising PEG macromonomers of different molecular weights (MW) and branching degrees and cross-linked them via click chemistry. Two different HIV-1 antigens were incorporated into the hydrogels either in their soluble form or attached to the surface of NPs.

2. Methods

2.1. Materials

All chemicals were purchased from Sigma Aldrich (Taufkirchen, Germany) f not stated otherwise. N-succinimidyl-3-maleimidopropionate was purchased from TCI EUROPE N.V. Sulfosuccinimidyl 4-(N-maleimidomethyl)cyclohexane-1-carboxylate (sulfo SMCC) and GibcoTM Phosphate buffered saline pH 7.4 (PBS; 1.5 mM KH_2PO_4, 8 mM Na_2HPO_4, 2.7 mM KCl, and 138 mM NaCl) were obtained from Thermo Fisher Scientific (Schwerte, Germany). Eight-armed PEG (8armPEG) with a hexaglycerol core and a MW of 10, 20, and 40 kDa and four-armed PEG (4armPEG) with a MW of 40 kDa were purchased from JenKem Technology (Allen, TX, USA). 100 nm silica NPs (SiNPs) functionalized with 1 μmol/g amino groups (sicastar® and sicastar® greenF, 25 mg/mL in water) were delivered by micromod Partikeltechnologie (Rostock, Germany). Broadly neutralizing antibody VRC01 was in-house produced and fluorescently labeled with a DY-647P1-NHS-Ester dye (Dyomics, Jena, Germany) using N-Hydroxy succinimide (NHS)–ester chemistry, as previously described (Peterhoff et al., 2022). HIV-1 envelope (Env) antigens were applied in a trimeric (Env_{tri}) and a monomeric (Env_{mono}) form and were expressed, purified, and characterized according to previously published protocol (Peterhoff et al., 2021a). Alexa647 labeled Env_{tri} was obtained by NHS–ester chemistry, according to a Nanotemper labeling protocol as previously described (Peterhoff et al., 2022). Ultrapure water was obtained from a Milli-Q water purification system (Millipore, Schwalbach, Germany).

2.2. Synthesis of macromonomers

Scheme 1 shows an overview of synthesized PEG macromonomers.

2.2.1. Synthesis of branched PEG-amines

8armPEG10K/20 K/40 K-NH_2, and 4armPEG40K-NH_2, were synthesized as described previously considering the MW and the branching degree (8arm or 4arm) of the polymers (Kirchhof et al., 2013).

2.2.2. Synthesis of 8armPEG10K/20 K/40 K-furan and 4armPEG40K-furan

The end-groups of 8armPEG10K/20 K/40 K-NH_2 and 4armPEG40K-NH_2 were functionalized with furyl groups (8armPEG10K/20 K/40 K-Furan and 4armPEG40K-Furan) considering the MW and the branching degree (8arm or 4 arm) of the polymers as previously described (Kirchhof et al., 2013).

2.2.3. Synthesis of 8armPEG10K/20 K/40 K-maleimide and 4armPEG40K

Exemplary the synthesis for 8armPEG10K is described. 8armPEG10K-NH_2 (3 g), 3 N-succinimidyl 3-maleimidopropionate (1.5-fold molar excess), and triethylamine (1.5-fold molar excess) were dissolved in 45 mL acetonitrile. After checking the pH (neutral) the solution was heated to 85 °C under reflux for 2 h, followed by 10 h stirring at room temperature. The solvent was evaporated under reduced pressure. The residue was dissolved in 150 mL water. The aqueous solution was extracted with DCM (3x 170 mL) and the pooled organic layers were dried with anhydrous Na_2SO_4 and further concentrated to 15 mL under reduced pressure. Finally, the product was precipitated (0 °C) by adding 300 mL of diethyl ether dropwise while vigorously stirring. The precipitate was filtered off, washed with cold diethyl ether, and vacuum-dried.

2.2.4. Synthesis of 4armPEG40K-Lys-AHX-Furan$_2$ and 4armPEG40K-Lys-AHX-maleimide$_2$

4armPEG40K-Lys-AHX-furan$_2$ was synthesized according to the protocol of Kirchhof et al. for 8armPEG20K-Lys-AHX-furan$_2$ considering the MW (40 kDa) and the branching degree (4arm) of the polymer (Kirchhof et al., 2015b). 4armPEG40K-Lys-AHX-maleimide$_2$ was

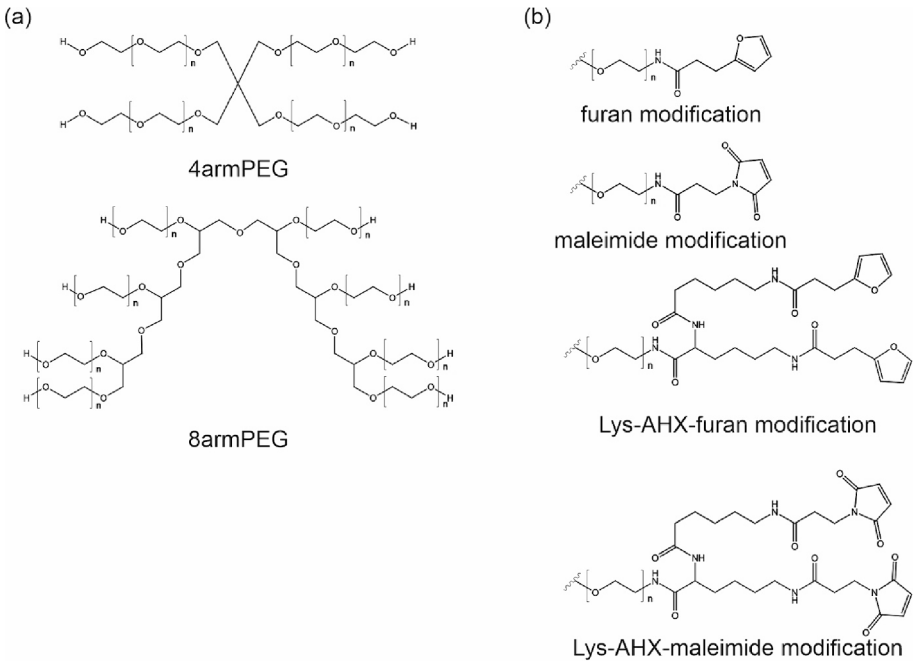

Scheme 1. (a) Chemical structures of multi-armed macromonomers used for synthesis of hydrogel precursors and (b) realized end-group functionalities. 8armPEG was used with a MW of 10, 20, or 40 kDa. For 4armPEG hydrogel precursors, macromonomers had a MW of 40 kDa.

synthesized in accordance to (Kirchhof et al., 2015b), with the exception, that for the last step 4armPEG40K-Lys-AHX-NH_2 reacted with N-succinimidyl 3-maleimidopropionate under water-free conditions to get the maleimide functionalization as reported in section 2.2.3. considering the branching degree and the MW of the macromonomer.

2.2.5. ^1H nuclear magnetic resonance (NMR) spectroscopy

To calculate the end group conversion, NMR spectra were taken in $CDCl_3$ using a Bruker Avance III 400 spectrometer (Bruker BioSpin GmbH, Rheinstetten, Germany). The integrated proton peak of each functional group was compared with the integrated PEG proton peak at δ 3.75–3.35 ppm. The conversion of the end groups ranged between 74–79 % for maleimide and 82–100 % for furan, respectively. For a detailed list of achieved end-group conversions, please refer to supporting information (SI; Table S1).

2.3. Attachment of antigen to silica NPs

We chose solid, amino functionalized (1 μmol/g) SiNP as basis for our antigen decorated NPs. SiNPs are well established in our laboratory and already successfully applied to augment the immune response against the HIV-1 Env protein and other antigens (Barbey et al., 2023; Peterhoff et al., 2021b; Thalhauser and Breunig, 2020; Thalhauser et al., 2020b). SiNPs carrying Env_{tri} (Env_{tri}-SiNPs) or Env_{mono} (Env_{mono}-SiNPs) were prepared as previously described (Peterhoff et al., 2021a; Thalhauser and Breunig, 2020; Thalhauser et al., 2020b). Briefly, aliquots of amino-functionalized SiNPs were adjusted to a concentration of 12.5 mg/mL (Env_{tri}) and 10 mg/mL (Env_{mono}), respectively, in 0.1 x phosphate buffered saline (PBS; 15 mM, pH 7.4). The particles were activated by a molar excess of bifunctional SMCC linker and allowed to react for 1 h. Afterwards, excess cross-linker was removed by centrifugation and redispersed in PBS (pH 6.7). Antigen, that was previously treated with 0.5 mM tris-(2-carboxyethyl)-phosphine was added to the NP suspension (antigen to NH_2 molar ratio of SiNP: Env_{mono} = 1:3; Env_{tri} = 1:1). The mixture was allowed to react over night at RT. Afterwards, the reaction was quenched by adding a molar excess of 2-mercapto ethanol, particles were washed three times with 0.1 x PBS, and redispersed in ultrapure water for a final concentration of 5 mg/mL (Env_{tri}) and 10 mg/mL (Env_{mono}) SiNP, respectively. Finally, the amount of bound antigen was determined using a QuantiPro™ BCA Assay Kit following the manufacturer's instructions, and the NP suspension was adjusted to a final antigen concentration of 1 mg/mL. The procedure was the same for green fluorescing solid SiNPs (sicastar® greenF; micromod Partikeltechnologie, Rostock, Germany).

2.4. NP characterization

The hydrodynamic diameter of the NPs was determined by dynamic light scattering (DLS) using a Malvern Zetasizer Nano ZS (Malvern, Herrenberg, Germany). For the DLS measurements, the NP stock solutions were diluted (1:10) and the general purpose mode with automatic measurement position was used. The data were acquired using Malvern Zetasizer Software 7.11 (Malvern Instruments, Worcestershire, UK).

2.5. Hydrogel preparation

Macromonomers with similar MW and branching degree were used. Equal molar amounts of maleimide-functionalized PEG and furan-functionalized PEG were dissolved independently in water. For hydrogels loaded with soluble Env_{tri} or Env-SiNPs, furan-functionalized PEG was dissolved in Env-SiNPs or soluble Env_{tri} containing water (50 μg/mL). The final polymer concentrations ranged from 5 to 15 % (w/V). The two liquid precursor solutions were mixed to induce gel formation. Immediately after mixing, 200 μL of the mixture were pipetted into previously siliconized (Sigmacote®, according to manufacturer's instructions) cylindrical glass molds (7 mm inner diameter) and allowed to gel for 72 h at 37 °C, 95 % relative humidity, and 5 % CO_2. The hydrogel loading for each antigen was 10 μg. Scheme 2 shows the reaction between furan and maleimide-functionalized multiarmed PEGs.

2.6. Hydrogel characterization

2.6.1. Rheology

Rheological behavior of the hydrogels was determined by a Malvern Kinexus Lab + rheometer (Malvern, Kassel, Germany) with a 25 mm parallel plate geometry as previously described (Ziegler et al., 2022;

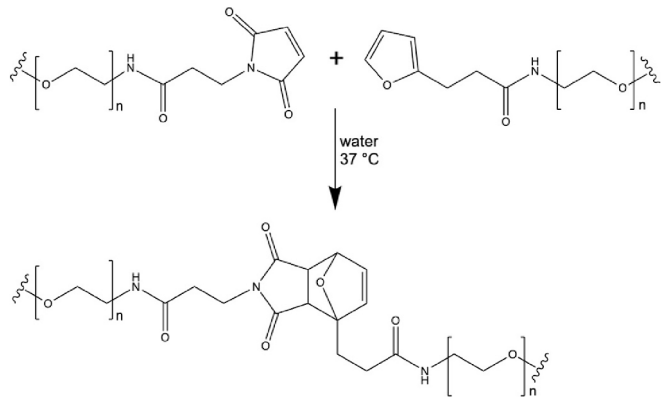

Scheme 2. Diels-Alder reaction, which underlies the cross-linking between maleimide and furan-functionalized PEG to create a hydrogel scaffold. This reaction takes place in water at 37 °C. Only one arm of the multiarmed macromonomers is shown for clarity.

Ziegler et al., 2021). The oscillation frequency was set to 1 Hz, and a strain of 1 % was applied. Monitored were storage (G′), loss (G″), and complex shear modulus (G*; a measure for hydrogel stiffness) over time. As gel point the cross-over point of G′ and G″, indicating the transition from a liquid-like to a solid-like behavior, was consulted. The final value of G* was determined after 2.5 h.

2.6.2. Hydrogel swelling and degradation

Empty hydrogel cylinders were manufactured as described in section 2.5. without addition of NPs. After gelling, hydrogels were weighed and immersed in 5 mL 50 mM PBS (pH 7.4) and incubated in a shaking water bath (10 rpm; 37 °C). At predefined timepoints, hydrogel mass was determined, and the hydrogels were subsequently incubated again in fresh buffer. Gel degradation was considered complete when macroscopic gel residues were no longer detectable.

2.6.3. Determination of the average mesh sizes (ξ_{avg}) of the hydrogels

Empty hydrogels cylinders were manufactured as described in section 2.5. Then, the hydrogel average mesh sizes were determined using the equilibrium swelling theory, as previously described (Kirchhof et al., 2013; Ziegler et al., 2021).

2.7. Antigen PEGylation

Maleimide reacts beside furan also with functional groups of amino acids such as primary amines or thiols [e.g. cysteine (cys)]. To investigate the extent of undesired reactions of maleimide to antigens as well as the impact of PEGylation on antigen integrity and functionality, conditions mimicking hydrogel formation were simulated. Therefore, particulate as well as soluble antigen was incubated with either short linear or multi-armed maleimide-functionalized PEG for 24 h at 37 °C. Afterwards samples were analyzed by HPLC (Figure S3), nano Differential Scanning Fluorimetry (nanoDSF), and microscale thermophoresis (MST).

2.8. Thermal stability measurements after antigen PEGylation

To investigate the impact of maleimide caused PEGylation on antigen conformity stability and integrity, thermal unfolding experiments using nanoDSF of soluble and particulate Env_{tri}, before and after incubation with linear (mPEG5K-maleimide) or branched PEG (8arm-PEG10K-maleimide), were performed. Therefore, soluble Env_{tri} and Env_{tri}-SiNPs at a final Env_{tri} concentration of 1.5 μM were incubated in PBS for 24 h at 37 °C with mPEG5K-maleimide (linear PEG) or 8arm-PEG10K-maleimide (branched PEG) at a final concentration of 150 and 5,000 μM, respectively. These concentrations correspond to a 100-fold and 26,666-fold molar excess of maleimide, respectively. Samples were used without further dilution. 10 μL of each sample was transferred into UV capillaries (Nanotemper Technologies, Munich, Germany) and experiments were performed using the Prometheus NT.48 device (Nanotemper Technologies, Munich, Germany). As temperature gradient, 1 °C/min (20 to 90 °C) was used. Protein unfolding was determined by detecting the temperature-dependent change in tryptophan fluorescence at emission wavelengths of 330 and 350 nm. The maximum of the first derivative of the fluorescence ratios (F330/F350) were detected which corresponds to the characteristic thermal unfolding transition midpoints (T_m). Data are presented as mean, based on the results of two independent samples.

2.9. Binding studies

To assess the functionality of soluble and particle bound Env_{tri} and Env_{mono}, respectively, after they were PEGylated with linear PEG macromonomer or released from hydrogels, antigens were probed with broadly neutralizing antibody VRC01 using microscale thermophoresis (MST) as described previously (Di Lorenzo and Seiffert, 2015). In brief, for the PEGylation experiments, soluble Env and Env-SiNPs at a final antigen concentration of 2.33 μM were incubated in PBS for 24 h at 37 °C with linear PEG (mPEG5K-maleimide) at a 100-fold molar excess of maleimide. As negative control served mPEG5k-maleimide incubated without soluble Env or Env-SiNP (data are not shown, since no binding occurred). For the MST measurements after Env-SiNPs were released from hydrogel, supernatants were collected without further processing. Prior to the MST measurements, the antigen concentration in the samples was adjusted to 400 nM using PBS containing polysorbate 20 (0.05 % (w/V)). Afterwards, multiple dilutions (1:1 V/V) of soluble Env or Env-SiNPs were prepared and mixed with an equal volume of labelled antibody. This resulted in Env concentrations ranging from 0.006 to 200 nM. The final antibody concentration for the measurements was 0.5 nM. Samples were examined using the Monolith NT 115 (Nanotemper Technologies, Munich, Germany) at room temperature. The excitation power was adjusted between 5 and 17 %, and MST power was set to 80 %. Three independent measurements were performed. Curve fits and resulting K_d values were obtained from the MO. Affinity Analysis software (NanoTemper; version 2.3).

2.10. Release studies

For release experiments, hydrogels were loaded with Env decorated green-fluorescing SiNPs (Env-SiNP-greenF) or soluble Env_{tri}-AF647. The amount of antigen per hydrogel was 10 μg. The resulting hydrogel cylinders were incubated in 3 mL of 50 mM PBS (pH 7.4) in a shaking water bath (10 rpm; 37 °C). Samples of 200 μL were withdrawn at regular timepoints and substituted with fresh buffer. The samples were stored at 4 °C until completion of the release experiment. The amount of released Env-SiNPs-FITC (λ_{ex} = 480 nm and λ_{em} = 520 nm) was determined on a FluoStar Omega plate reader (BMG Labtech, Ortenberg, Germany) using a calibration curve prepared with SiNPs-greenF (ranging from 0 to 200 μg/mL) or Env-SiNP-greenF (ranging from 0 to 3 μg/mL related to protein content). The amount of released soluble Env_{tri}-AF647 (λ_{ex} = 594 nm and λ_{em} = 633 nm) was determined on a Synergy Neo2 (BioTek Instruments, Winooski, VT, U.S.) using a calibration curve of Env_{tri}-AF647 ranging from 0 to 3 μg/mL. For a better comparability and illustration, data are presented as normalized cumulative release.

2.11. Statistical analysis

If not otherwise stated, all experiments were performed at least in triplicate and the results are presented as means ± standard deviations. Two-way ANOVA, followed by Tukey's multiple comparisons test (Fig. 2b) and Sidak's multiple comparisons test (Fig. 3b), respectively, were performed using GraphPad Prism 8.3.0 (GraphPad Software Inc.,

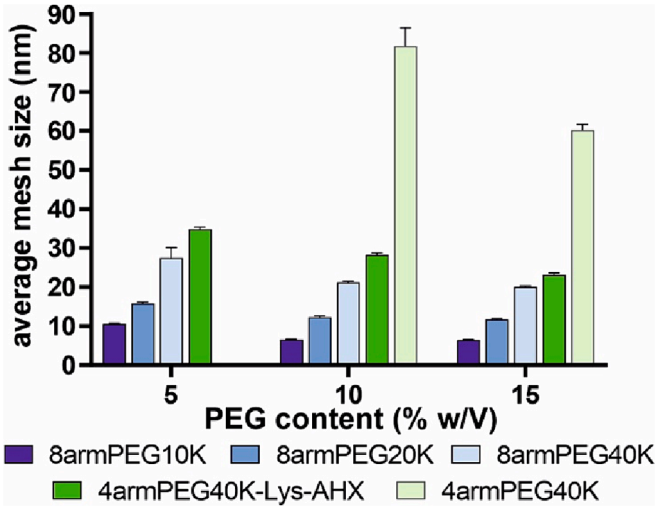

Fig. 1. Average mesh sizes (ξ_{avg}) of different hydrogels (of 5, 10, and 15 % (w/V)) are shown. The average mesh size (nm) of the hydrogels were determined using the equilibrium swelling theory as described previously (Kirchhof et al., 2013; Ziegler et al., 2021). Data are expressed as mean ± standard deviation of three different hydrogel cylinders. Further hydrogel characteristics are shown in Figure S2.

La Jolla, CA, USA) to assess statistical significance.

3. Results

3.1. Platform of PEG hydrogels to allow for the release of antigen-decorated SiNPs

We developed a PEG based hydrogel platform to allow for the sustained release of antigen-decorated nanoparticles. 8arm and 4armPEG macromonomers were chosen as building blocks to be cross-linked via the Diels-Alder "click" reaction to fabricate an 8armPEG and a 4armPEG hydrogel series (Scheme 3). For the 8armPEG series, macromonomers were used in three different MWs of 10, 20, and 40 kDa, and were successfully modified with either furyl or maleimide functionalities resulting in the following hydrogel nomenclature: 8armPEG10K, 8armPEG20K, and 8armPEG40K. For the 4armPEG series, only a MW of 40 kDa was applied. Here, furyl or maleimide functionalities were either directly attached to the PEG macromonomeŕs distal ends or to the PEG macromonomer that have been previously modified with a branched hydrophobic two-arm spacer (Lys-AHX) resulting in the following hydrogel nomenclature: 4armPEG40K and 4armPEG40K-Lys-AHX, respectively. For details of conversion and yields, please refer to SI (Table S1).

HIV-1 envelope (Env) antigens were covalently attached to the surface of SiNPs. The resulting Env-SiNPs were incorporated into the hydrogel during gel formation (Scheme 3). The Env antigen was applied either in a trimeric (Env_{tri}) or a monomeric (Env_{mono}) form, respectively (Table 1). Env_{tri} has a MW of about 215 kDa. Leaving aside the additional size contribution due to glycosylation in the range of 100 kDa (Bender et al., 2021), the protein has a predicted hydrodynamic diameter of ~7.9 nm. Env_{mono} involves the small receptor-binding domain of one monomer of the Env_{tri} and is also glycosylated. It has a MW of about 42.5 kDa which corresponds to a hydrodynamic diameter of ~4.6 nm. Both particle types, Env_{tri}-SiNPs and Env_{mono}-SiNPs, had a similar hydrodynamic diameter of about 150 nm. The polydispersity index (PDI) of both particle types was below 0.2, indicating a monodisperse size distribution. About 168 Env_{mono} and 266 Env_{tri}, respectively, were covalently attached to one SiNP.

3.2. Hydrogels have several possibilities to tailor physical properties

The gelation time (t_{gel}) of the hydrogel, which indicates the transition from a liquid- to a solid-like behavior, was determined. In the 8armPEG hydrogel series, the t_{gel} decreased with decreasing MW of the polymer from about 83 to 34 min. Comparing the PEG hydrogels that were fabricated with the 40 kDa macromonomers, the 8armPEG40K gelled with about 83 min much faster than 4armPEG40K with about 302 min. Interestingly, by introducing the branched two-arm spacer to the 4armPEG40K, the gelation time accelerated from about 302 min to about 60 min (Table 2).

To get an idea of the maximal possible release timeframes of incorporated SiNPs, minimal dissolution time ($diss_{min}$) of all hydrogel types was determined. In the series of the 8armPEG hydrogels, the minimal dissolution time decreased with increasing MW from about 15 to 36 days. For the 4armPEG hydrogel series, the minimal dissolution time increased with the introduction of the hydrophobic spacer from 2 to 46 days (Table 2).

Since the hydrogel mesh size could also have an impact on release kinetics and duration of nanoparticle release, Fig. 1 shows the average mesh size (ξ_{avg}) of each hydrogel type at three different polymer concentrations. Generally, with increasing polymer concentration from 5 to 15 % (w/V), the average mesh size of the hydrogels decreased. Comparing the five different hydrogel types at the same polymer concentration of 10 % (w/V), the average mesh size was as follows: in the 8armPEG hydrogel series the mesh size increased with increasing MW from about 6 to 20 nm. For the 4armPEG hydrogel series the average mesh size decreased with the introduction of the hydrophobic two-arm spacer from about 82 to 35 nm. Importantly, incorporation of antigen-SiNPs in hydrogels had no great impact on gelation time and hydrogel strength (Figure S2).

3.3. Hydrogel components have no impact on antigen integrity and functionality

Because the hydrogel formation involves a covalent cross-linking step, it could have a potential impact on antigen integrity and functionality. Since analysis of these parameters is highly challenging in a complex matrix like a hydrogel, soluble Env as well as Env-SiNPs were incubated with maleimide-functionalized PEG macromonomers to emulate the scenario during hydrogel formation. The conformational stability of Env_{tri} in its soluble form and attached to SiNPs was then determined by the characteristic thermal unfolding transition midpoint (T_m) in the presence and absence of PEG (Fig. 2a). Hardly any effect on T_m of both soluble Env_{tri} as well as Env_{tri}-SiNPs was detected after the treatment with both PEG types. Only the T_m of Env_{tri} was slightly higher after the incubation with branched PEG.

Antigen integrity and functionality after incubation with linear PEG were additionally investigated by binding studies of the VRC01 antibody to the antigens. VRC01 is one of the most potent broadly neutralizing antibodies and binds specifically to the CD4 binding site of Env. A successful binding of VRC01 to Env is thus a good indication for antigen integrity and functionality. Fig. 2b shows the binding affinity (K_d values) of antigens before and after PEGylation. For Env_{mono}, the K_d values of VRC01 to Env_{mono} and Env_{mono}-SiNPs were similar with about 2.5 and 2.2 nM, respectively. Both Env_{mono} and Env_{mono}-SiNPs were not significantly affected by PEGylation because the K_d values only slightly increased. For Env_{tri}, the K_d values of VRC01 to Env_{tri} and Env_{tri}-SiNPs were about 38.3 and 7.8 nM, respectively. This significant difference ($P = <0.0001$) between soluble and particulate Env_{tri} was expected because the particulate Env_{tri} allow for a multivalent binding of the VRC01 resulting in an avidity gain (Thalhauser et al., 2020a). Again, both soluble Env_{tri} and Env_{tri}-SiNPs were not significantly affected by PEGylation.

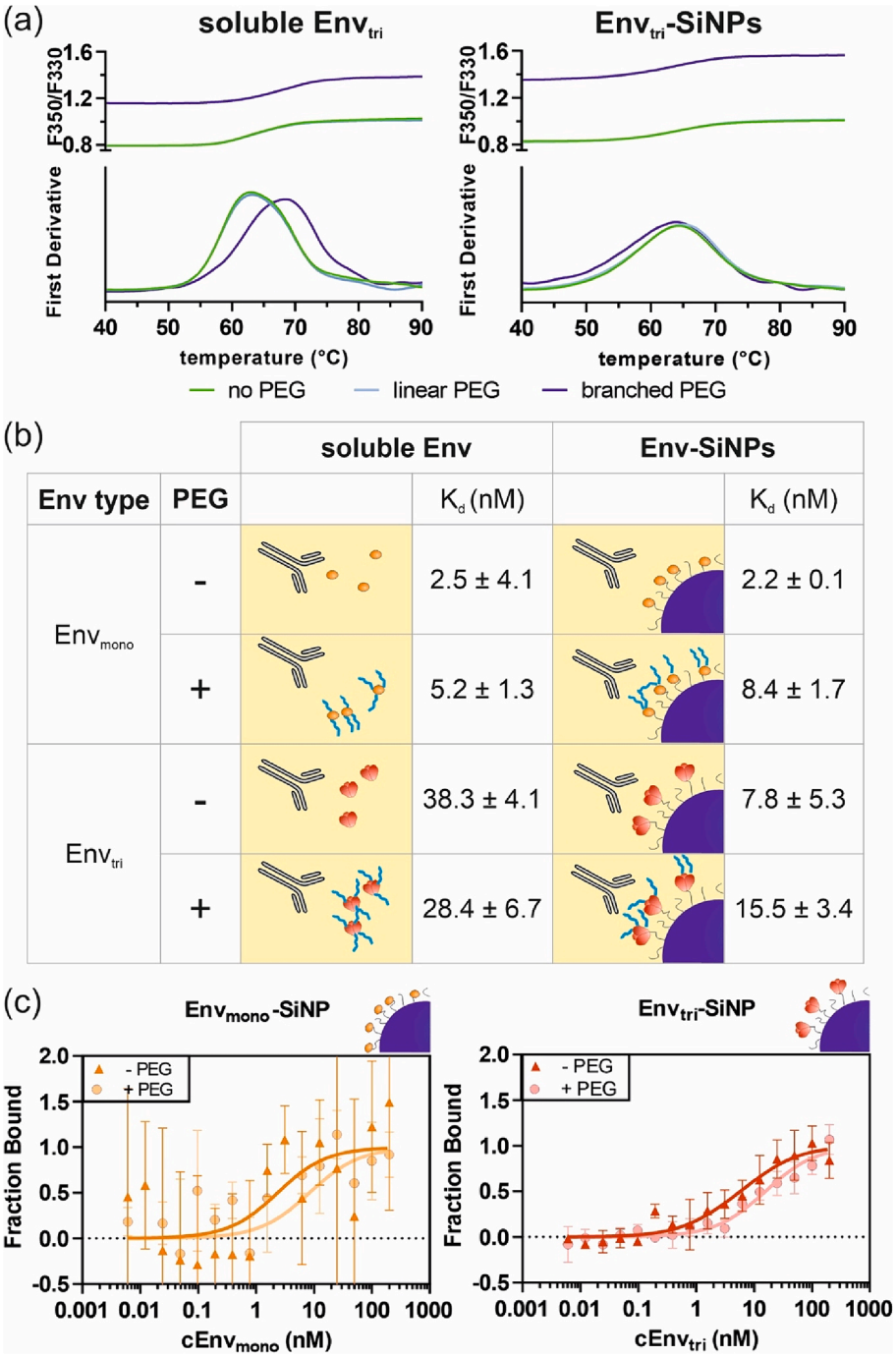

Fig. 2. Integrity and functionality of Env after incubation with hydrogel precursors. (a) Thermostability of soluble Env$_{tri}$ as well as particulate Env$_{tri}$-SiNP before and after incubation with linear (mPEG5K-maleimide) or branched (8armPEG10K-maleimide) PEG macromonomers. Presented is the characteristic temperature-dependent change in tryptophan fluorescence ratio of emission wavelengths (F330/F350). Unfolding transition midpoints (T_m) were determined by detecting the maximum of the first derivative of the fluorescence ratios (curves below). (b) Presented are K_d values (nM) determined by measuring the binding affinity of broadly neutralizing antibody VRC01 to soluble Env$_{tri}$ and Env$_{mono}$ as well as Env$_{tri}$-SiNPs and Env$_{mono}$-SiNPs before and after incubation with maleimide-functionalized linear PEG. As negative control served mPEG5k-maleimde incubated without soluble Env or Env-SiNP (data are not shown, since no binding occurred). Data are expressed as mean ± standard deviation. (c) Exemplary antibody binding curves of the VRC01 to non-PEGylated and PEGylated Env$_{mono}$-SiNP as well as Env$_{tri}$-SiNP are shown. Data curves served as a calculation basis of the corresponding K_d values. Further binding curves are shown in Figure S4a-b.

3.4. Release of antigen decorated SiNPs from PEG hydrogels can be tailored while maintaining their functionality

The release of Env-SiNPs from hydrogels was influenced by the MW and the branching of the PEG macromonomers (Fig. 3a). In the 8armPEG hydrogel series, the release duration decreased from about 40 to about 30 days with increasing MW. Irrespective of the MW, all 8armPEG hydrogels showed a similar biphasic release profile with a faster initial release followed by a sustained release. The release of the SiNPs was not affected by the antigen type on SiNPs because the release curves of Env$_{mono}$-SiNPs and Env$_{tri}$-SiNPs were nearly on top of the other. The 4armPEG40K hydrogel released Env-SiNPs within the very short time-frame of two days. The introduction of the two-arm spacer prolonged the release up to 50 days. Again, no differences between Env$_{tri}$-SiNPs and

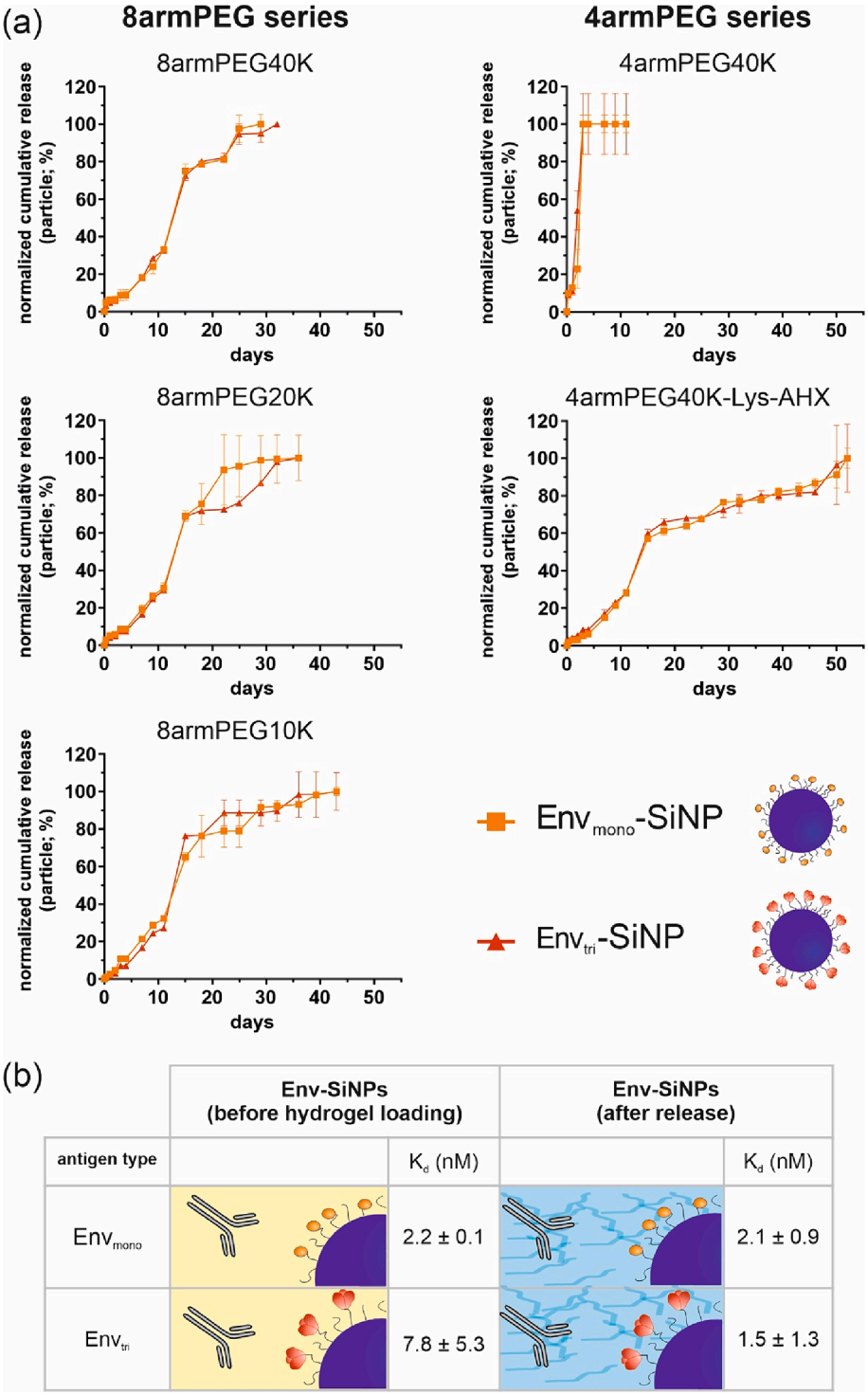

(b)

antigen type	Env-SiNPs (before hydrogel loading) K_d (nM)	Env-SiNPs (after release) K_d (nM)
Env_{mono}	2.2 ± 0.1	2.1 ± 0.9
Env_{tri}	7.8 ± 5.3	1.5 ± 1.3

Fig. 3. Release of Env-SiNPs from PEG hydrogels and their functionality after release. (a) Cumulative release of Env_{mono}- and Env_{tri}-SiNPs from 8arm and 4arm hydrogel series. Release experiments were performed in PBS at 37 °C. For all hydrogels, the polymer concentration was 10 % (w/V). Data are expressed as mean ± standard deviation of three independent hydrogel cylinders. (b) Presented are K_d values (nM) determined by measuring the binding affinity of broadly neutralizing antibody VRC01 to Env_{tri}-SiNPs as well as Env_{mono}-SiNPs before hydrogel loading and after release via MST. As exemplary hydrogel 4armPEG40K (10 % (w/V)) was used. Data are expressed as mean ± standard deviation. The corresponding binding curves are shown in Figure S4c.

Env_{mono}-SiNPs were detected.

Functionality of released Env-SiNPs was confirmed by comparing K_d values of VCR01 to Env-SiNP before hydrogel loading and after release (Fig. 3b). The K_d values of VRC01 to Env_{mono}-SiNP before and after release were similar with about 2.2 and 2.1 nM, respectively. The K_d value of VRC01 to Env_{tri}-SiNP was significantly ($P = 0.0466$) improved after release from about 7.8 to 1.5 nM. The corresponding binding curves are shown in Figure S4c.

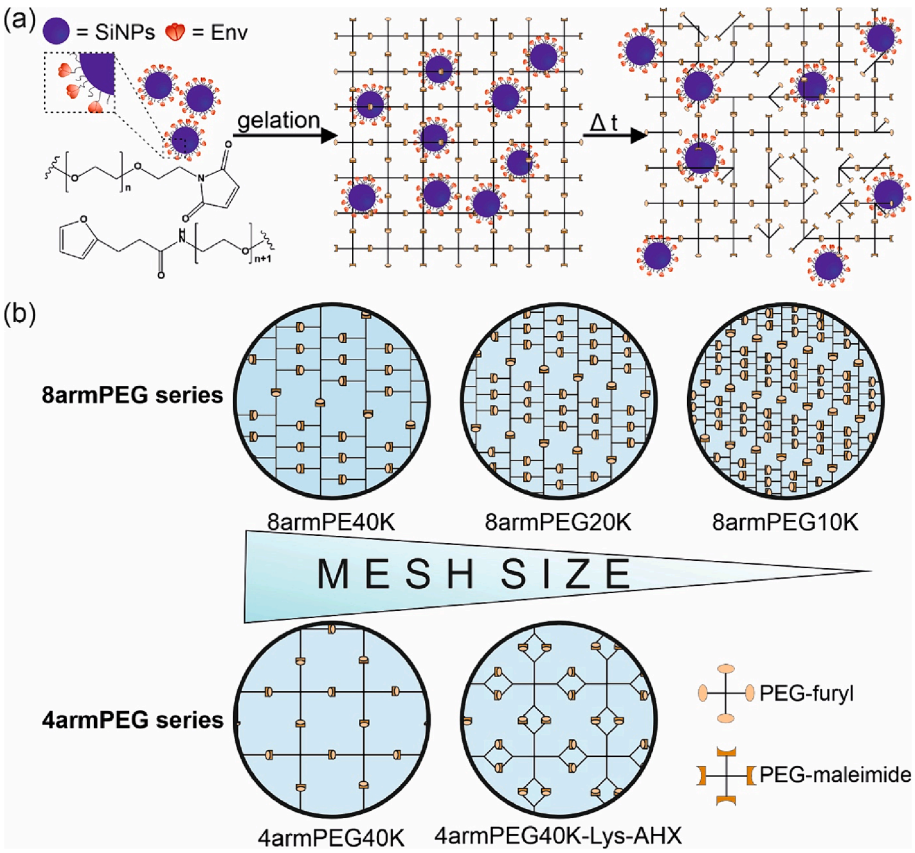

Scheme 3. Hydrogel preparation and overview of hydrogel types. (a) Maleimide- and furan-functionalized branched PEG macromonomers were mixed with antigen-SiNPs, and hydrogels cylinders (200 μL; 7 mm of diameter and 5.2 mm in height) were formed. Antigen-SiNPs are envisioned to be released by hydrogel swelling and degradation. (b) An 8arm and a 4armPEG hydrogel series was realized. Depending on the MW of PEG macromonomers and the branching degree (8arm or 4arm), hydrogels of different mesh sizes were obtained.

Table 1
Properties of soluble Env and Env-SiNPs.

Env type	Env_{mono}	Env_{tri}	**Number of Env/SiNP**	168	266
MW (kDa)	42.5	215	**Size**[b] **(nm)**	138.1 ± 2.5	157.6 ± 2.8
Size[a] **(nm)**	4.6	7.9	**PDI**[c]	0.11 ± 0.01	0.15 ± 0.01

[a] Hydrodynamic diameter; values were predicted according to previous publication (Erickson, 2009).
[b] Hydrodynamic diameter; determined by dynamic light scattering.
[c] PDI = polydispersity index.

Table 2
Polymer and hydrogel characteristics. Overview of polymer and hydrogel properties such as molecular weight (MW) of macromonomers, gelation time (t_{gel}) and minimal dissolution time ($diss_{min}$) of hydrogels at a polymer concentration of 10 % (w/V). Data are expressed as mean ± standard deviation of three different hydrogel cylinders.

Polymer type	**MW (kDa)**	**t_{gel} (min)**	**$diss_{min}$ (days)**
8armPEG40K	40	83.4 ± 1.9	15
8armPEG20K	20	46.0 ± 1.9	23
8armPEG10K	10	34.3 ± 0.8	36
4armPEG40K	40	301.6 ± 35.0	2
4armPEG40K-Lys-AHX	40	60.3 ± 3.7	46

3.5. PEG hydrogels allow for the co-delivery of soluble and particulate antigen

To realize a potential vaccine formulation allowing for different immunization principles within one application, it might be of interest to release soluble Env and Env-SiNP antigen from one hydrogel. Because a long release timeframe is envisioned, we focused on the release of soluble Env_{tri} from 8armPEG10K and 8armPEG20K hydrogels (Fig. 4a). As expected, release duration of Env_{tri} increased with decreasing MW of the PEG macromonomers and increasing polymer concentration. In this way, the release duration could be modulated between 30 and 50 days. To compare the release duration and profile between soluble Env_{tri} and Env_{tri}-SiNPs, an overlay of both release curves from separate experiments is shown in Fig. 4b. Surprisingly, larger Env_{tri}-SiNPs were released

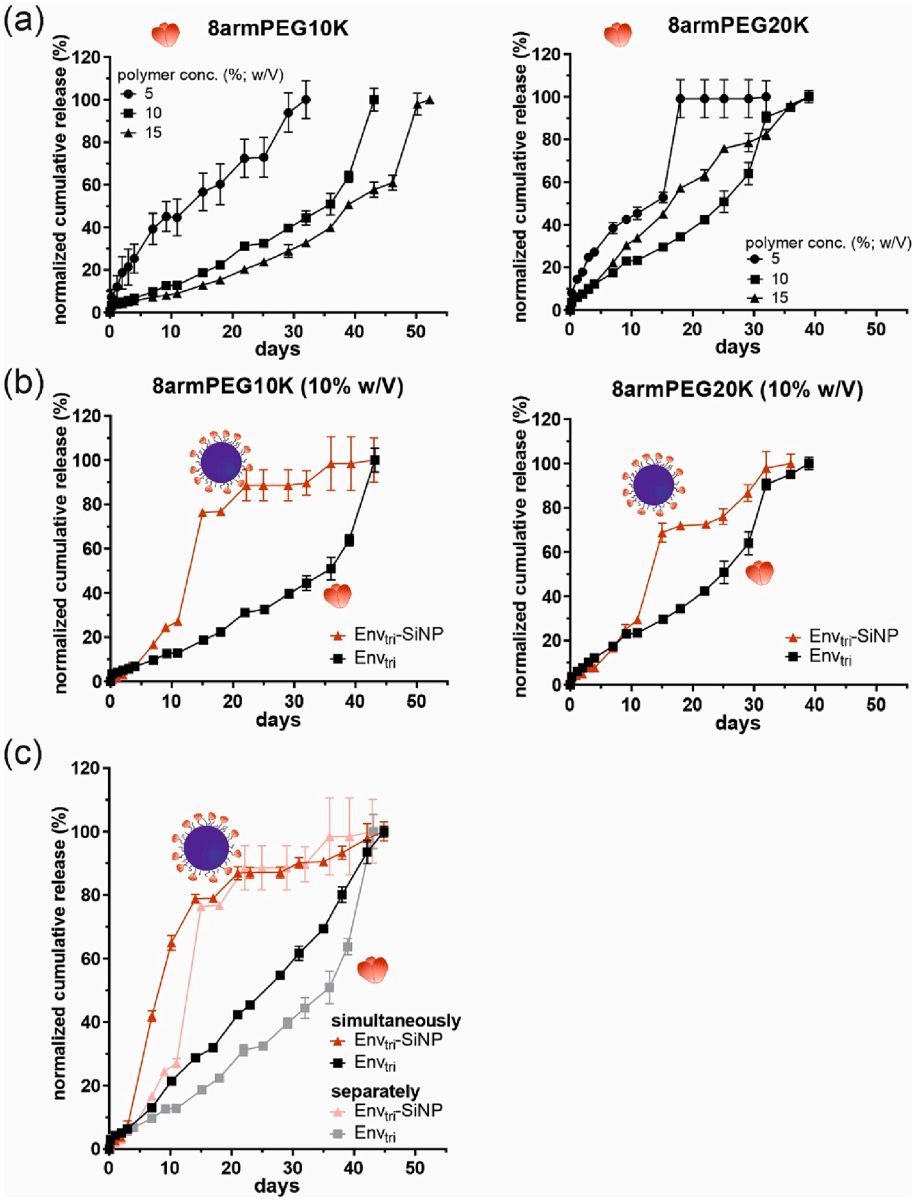

Fig. 4. Release of soluble Env$_{tri}$ and co-delivery of soluble Env$_{tri}$ and Env$_{tri}$-SiNPs. (a) Cumulative release of fluorescently labeled Env$_{tri}$ from 8armPEG10K and 20 K hydrogels of three different polymer concentrations (5, 10, 15 % (w/V)). (b) Presented is the overlay of cumulative release of soluble Env$_{tri}$ (black squares) and Env$_{tri}$-SiNPs (red triangles) from 8armPEG10K and 8armPEG20K hydrogel. (c) Shown is the overlay of separate (pale symbols) and co-delivery (saturated symbols) of Env$_{tri}$-SiNPs (red triangles) and soluble Env$_{tri}$ (black squares) from an 8armPEG10K hydrogel (10 % (w/V)).

faster than the smaller soluble Env$_{tri}$.

To evaluate if soluble Env$_{tri}$ and Env$_{tri}$-SiNPs mutually influence each other, we incorporated both species in one hydrogel for a co-delivery. The initially observed trend that larger particles are faster released than the soluble antigen was maintained. In comparison to the separate release, the total release timeframe of approximately 43 days did not changed. The particles were even released slightly faster at the initial phase, whereas the soluble Env showed a continuous release over the whole timeframe (Fig. 4c).

4. Discussion

A prolonged availability of antigens, which mimics the kinetics of a natural infection has gained great attention in vaccine design to improve long lasting immunity (Boopathy et al., 2019; Cirelli et al., 2019; Cirelli and Crotty, 2017a; Gale et al., 2021; Roth et al., 2020; Tam et al., 2016). Hydrogels are cross-linked networks with high water content (>90 %) and provide for a protein friendly environment for *in vivo* delivery of therapeutics (Wang et al., 2018). Therefore, we developed a PEG based hydrogel platform to allow for the sustained release of antigen decorated SiNPs. PEG is known for its excellent biocompatibility, chemical versatility, and its simplicity to functionalize, and was therefore chosen as building block for hydrogel formation via Diels-Alder click reaction (Dingels et al., 2011; Sun et al., 2023). A great advantage of the cross-linking reaction is the degradability of covalent bonds under physiological conditions via *retro*-Diels–Alder reaction (Kirchhof et al., 2015c). To get PEG hydrogels of different release characteristics and kinetics, an 8armPEG hydrogel series of different MWs (10, 20, and 40 kDa) and a 4armPEG hydrogel series of a MW of 40 kDa were end-group functionalized with furan and maleimide to allow for covalent cross-linking and hydrogel formation. To increase the stability of less branched hydrogels (i.e. 4armPEG40K), a two-arm hydrophobic spacer was introduced, thereby doubling the number of reactive end-groups to get dendritic macromonomers with improved hydrolytic stability (Kirchhof et al.,

2013). For the particulate antigen formulation, we chose aminated non-porous SiNPs with a size of 100 nm. SiNPs have already successfully been applied by us in several studies related to the development of an HIV-1 vaccine (Peterhoff et al., 2022; Peterhoff et al., 2021a; Thalhauser and Breunig, 2020; Thalhauser et al., 2020b, c). In addition, silicon-dioxide is generally recognized as safe by the FDA (Watermann and Brieger, 2017). Moreover, NP sizes below 200 nm are favorable in entering the lymphatics directly which is beneficial in terms of vaccination (Thalhauser et al., 2020a). Two different Env variants were attached to the surface of SiNPs: recombinant Env_{tri} (215 kDa) and a receptor-binding domain of Env_{tri} (Env_{mono}; 42.5 kDa). Despite the difference in MW, the hydrodynamic diameter of Env_{mono} and Env_{tri} decorated SiNPs were similar to each other and comparable to previously published data (Peterhoff et al., 2021a).

Prior to hydrogel formation, antigens are dissolved or dispersed in the hydrogel precursor solution and could thus potentially form PEG-antigen conjugates altering their structure or stability. The recombinantly expressed Env antigens carry cysteine (cys) tags for covalent attachment to the SiNP surface, which are easily accessible and prone to Michael-type reaction with maleimide-functionalized PEG. Besides these available cys tags, other cys of recombinant Env form disulfide bonds (Yuan et al., 2005) which are located mainly in inaccessible hydrophobic domains and present, thus, only low reactivity (Santos et al., 2018). Therefore, soluble Env_{mono} or Env_{tri} which have the cys tag still available, bear a higher risk to be PEGylated compared to Env_{mono} or Env_{tri} immobilized on SiNPs. At the same time, hydrogel formation is performed in ultrapure water, an environment known for a lower degree of PEGylation of proteins due to the slightly acid pH (Hammer et al., 2015). In our study, the stability of the soluble as well as the particulate Env was not affected by PEGylation, which is in good agreement with previous publications (Liu et al., 2022; Plesner et al., 2011). Xiao Liu et al., for example, observed that PEGylation did not alter the structure and thermodynamic stability of a protein (Liu et al., 2022). Protein PEGylation may be at the expense of their affinity for their specific binding site (Chan et al., 2016; Dhalluin et al., 2005; Kozma et al., 2020). Fortunately, the affinity of the VRC01 antibody that binds specifically to the CD4 binding site of soluble or particulate Env, was not negatively affected by PEGylation, indicating an intact and functional antigen. Most important, even after release of Env_{tri}-SiNPs and Env_{mono}-SiNPs from a PEG hydrogel the antibody affinity was not negatively affected, indicating that hydrogel formation and release have no negative impact on antigen functionality. Although the effect of antibody PEGylation on its interaction with its specific target antigen has already been extensively studied in the literature (Selis et al., 2016), to the best of our knowledge, the vice versa scenario, i.e., the affinity of an antibody to its PEGylated specific target antigen, has been poorly investigated yet. Although antigen functionality after release has been demonstrated *in vitro*, it still needs to be confirmed how well the epitopes are recognized by the immune system *in vivo*. Interestingly, PEGylation of a toll-like receptor-2-agonist-based vaccine delivery system improved antigen trafficking and the magnitude of ensuing antibody and CD8 + T cell responses (Sekiya et al., 2017).

The maximal release timeframe of Env-SiNPs is limited by the minimal dissolution time and, thus, by the stability of the hydrogels which depends on the MW and the branching degree of the polymer. This is related to the fact that the stability of hydrogels decreases with increasing polymer MW and decreasing branching degree (Kirchhof et al., 2013). On the other hand, the release kinetics depends on the average mesh size of the hydrogel and the hydrodynamic diameter of the embedded molecules (Ziegler et al., 2021). Since the size of Env-SiNPs is much larger than the initial average mesh size of the hydrogels, a strong retention of the SiNPs in the hydrogel matrix was expected. On the contrary, Env-SiNPs were released without major retention with an initial fast exponential like release followed by a slower release up to the end. An explanation may be that polymer based hydrogels have shown to contain areas of high cross-linking density and besides areas of low cross-linking density (Di Lorenzo and Seiffert, 2015). Therefore, the mesh size distribution of a hydrogel can thus be very wide. Since Env-SiNPs are very large in size relative to the hydrogel mesh size, we hypothesize, that Env-SiNPs are displaced from areas of high cross-linking density to areas of low cross-linking density due to their higher space requirement. Additionally, Env-SiNPs may sterically disrupt the hydrogel structure and presumably lead to further hydrogel defects, which finally leads to an increased nanoparticle mobility within the hydrogels after swelling and, thus, to a faster release. Support for this assumption comes from confocal microscopic images of hydrogel cross-sections loaded with Env-SiNPs showing that the particles are distributed inhomogeneous throughout the hydrogel (Figure S5). Additionally, hydrogel stiffness was slightly affected by the incorporation of antigen-SiNPs, indicating that NPs most likely disrupt the hydrogel scaffold (Figure S2c). But anyway, the initial exponential-like release mimicking natural infection could be beneficial in terms of immune response effectiveness since it was demonstrated that an exponentially increasing dosing of an antigen is superior compared to a constant exposure (Tam et al., 2016). Which release timeframe is ultimately most effective in triggering a strong immune response and most tolerable by the patient needs to be investigated *in vivo*. In addition, there is evidence that PEG based implants, despite their excellent biocompatibility, are associated with adverse effects like chronic inflammation which may lead to an inflammatory response triggering a foreign body reaction (Kastantin et al., 2011; Swartzlander et al., 2015). This could ultimately lead to the formation of a fibrous capsule surrounding the hydrogel. Because the formation of a fibrous barrier may take place not until about 30 days it may mainly hamper the release of Env-SiNPs from hydrogels with longer stability (Carnicer-Lombarte et al., 2021). This issue will be investigated in further *in vivo* experiments.

There is evidence that sequential heterologous immunization (vaccination schemes with vaccines based on different principles, e.g., the combination of RNA/DNA based with vector- or protein-based vaccines (Palgen et al., 2021)) over a longer period of time may shape B-cell maturation towards mature broadly neutralizing antibodies which are required for long lasting immunity (Peterhoff and Wagner, 2017). Therefore, it was reasonable to co-deliver soluble and particulate Env_{tri} from one hydrogel. Prior to co-delivery, the single release of soluble Env_{tri} was characterized. The sigmoidal release profile is probably related to the high MW of glycosylated Env_{tri} of around 315 kDa (Bender et al., 2021). A comparable sigmoidal but more pronounced release profile was observed by Kirchhof et al. releasing dextran with a MW of 500 kDa from a similar hydrogel (Kirchhof et al., 2015a). Interestingly, an expected burst release did not occur during the first 24 h and was limited to a maximum of about 5 %. This indicates a good entrapment of Env_{tri} by the hydrogel scaffold especially in areas of high cross-linking density which could be an explanation for the slower release compared to Env_{tri}-SiNPs. During co-delivery of soluble Env_{tri} and Env_{tri}-SiNPs from one hydrogel, both components were even slightly faster released compared to their release after entrapment in separate hydrogels. A possible reason could be that twice the amount of antigen is included per hydrogel, thereby increasing the number of molecular structures possibly interfering and loosening up the hydrogel scaffold. Interestingly, the overall release timeframe was independent if soluble Env_{tri} and Env_{tri}-SiNPs were released from one or two separate hydrogels. It must be kept in mind that a possible interaction between the two components – soluble Env_{tri} and Env_{tri}-SiNP- affecting their functionality still needs to be investigated in further studies. In terms of vaccination practice, it has been shown that prime/boost vaccine increases the magnitude and durability of HIV-specific CD4 T-cell responses (De Rose et al., 2015). This comprises an initial vaccination (prime) followed by an additional vaccination some weeks later (boost) (De Rose et al., 2015). Therefore, the co-delivery of soluble and particulate Env_{tri} seems to be reasonable: about 80 % of Env_{tri}-SiNPs are released during the first 12 days, while soluble antigen is constant released over 43 days. This may be beneficial because it has been demonstrated that sequential

heterologous immunization over a long period of time shape the B-cell maturation towards mature broadly neutralizing antibodies and long lasting immunity (Peterhoff and Wagner, 2017). Alternatively, or in addition to the soluble Env_{tri}, an adjuvant could also be co-delivered, which may enhance the antigen-specific immune response or influence the direction of the immune response (Wagner and Hildt, 2019).

5. Conclusion and outlook

We successfully developed a PEG based hydrogel platform allowing for controlled and sustained release of antigen decorated SiNPs mimicking natural infection kinetics over various timeframes. The integrity and functionality of antigens after release was successfully maintained. Additionally, the feasibility of co-delivering soluble and particulate antigen was demonstrated. Thus, in addition to the prolonged antigen presentation, our hydrogel formulation represents a kind of single-dose sequential vaccine with the potential to combine a prime-boost vaccine in one application. Such a vaccine administration could reduce costs, potentially increase vaccine coverage, and simplify the logistics compared to multidose vaccine administration especially in low- and middle-income countries (Barnabas et al., 2022).

Funding

This paper is accrued as part of the research project "**HI**V **Vac**cine **T**argeting via DNA **O**rigami Nanoparticles to lymph nodes to promote **G**erminal **C**enter formation (**HIVacToGC**)". This project has received funding from the Federal Ministry of Education and Research, Germany (BMBF) as part of program "Gezielter Wirkstofftransport" (funding code 16GW0363K).

CRediT authorship contribution statement

Raphael Mietzner: Writing – review & editing, Writing – original draft, Visualization, Validation, Project administration, Methodology, Investigation, Formal analysis, Data curation, Conceptualization. **Clara Barbey:** Writing – review & editing, Formal analysis, Data curation. **Heike Lehr:** Writing – review & editing, Methodology. **Christian E. Ziegler:** Writing – review & editing, Methodology. **David Peterhoff:** Writing – review & editing, Resources. **Ralf Wagner:** Writing – review & editing, Project administration, Funding acquisition, Resources. **Achim Goepferich:** Writing – review & editing, Project administration, Conceptualization, Resources. **Miriam Breunig:** Writing – review & editing, Supervision, Resources, Project administration, Investigation, Funding acquisition, Conceptualization.

Declaration of competing interest

The authors declare that they have no known competing financial interests or personal relationships that could have appeared to influence the work reported in this paper.

Data availability

Data will be made available on request.

Acknowledgment

The authors thank the German Federal Ministry of Education and Research, Germany (BMBF; grant No 16GW0363K) for the support that made this project possible. The authors thank Renate Liebl, Silvia Babl, Chrismarie Faltermaier, Merve Goekalp, and Nadine Stefan for their excellent technical support. The authors acknowledge Prof. Gernot Laengst for the opportunity to use the MST device and the team from 2bind for their scientific support and the opportunity to use their Prometheus NT.48. Furthermore, the authors thank Felix Baumann and Johannes Konrad for scientific input, and Carsten Damm for proofreading.

Appendix A. Supplementary material

Supplementary data to this article can be found online at https://doi.org/10.1016/j.ijpharm.2024.124131.

References

Barbey, C., Su, J., Billmeier, M., Stefan, N., Bester, R., Carnell, G., Temperton, N., Heeney, J., Protzer, U., Breunig, M., Wagner, R., Peterhoff, D., 2023. Immunogenicity of a silica nanoparticle-based SARS-CoV-2 vaccine in mice. Eur. J. Pharm. Biopharm. 192, 41–55.

Barnabas, R.V., Brown, E.R., Onono, M.A., Bukusi, E.A., Njoroge, B., Winer, R.L., Galloway, D.A., Pinder, L.F., Donnell, D., Wakhungu, I., Congo, O., Biwott, C., Kimanthi, S., Oluoch, L., Heller, K.B., Leingang, H., Morrison, S., Rechkina, E., Cherne, S., Schaafsma, T.T., McClelland, R.S., Celum, C., Baeten, J.M., Mugo, N., 2022. Efficacy of single-dose HPV vaccination among young African women. NEJM Evid 1, EVIDoa2100056.

Bender, M.F., Li, Y., Ivleva, V.B., Gowetski, D.B., Paula Lei, Q., 2021. Protein and glycan molecular weight determination of highly glycosylated HIV-1 envelope trimers by HPSEC-MALS. Vaccine 39, 3650–3654.

Boopathy, A.V., Mandal, A., Kulp, D.W., Menis, S., Bennett, N.R., Watkins, H.C., Wang, W., Martin, J.T., Thai, N.T., He, Y., Schief, W.R., Hammond, P.T., Irvine, D.J., 2019. Enhancing humoral immunity via sustained-release implantable microneedle patch vaccination. Proc. Natl. Acad. Sci. 116, 16473–16478.

Brandl, F., Hammer, N., Blunk, T., Tessmar, J., Goepferich, A., 2010. Biodegradable hydrogels for time-controlled release of tethered peptides or proteins. Biomacromolecules 11, 496–504.

Brinkkemper, M., Sliepen, K., 2019. Nanoparticle vaccines for inducing HIV-1 neutralizing antibodies. Vaccines 7, 76.

Brouwer, P.J.M., Sanders, R.W., 2019. Presentation of HIV-1 envelope glycoprotein trimers on diverse nanoparticle platforms. Curr. Opin. HIV AIDS 14, 302–308.

Carnicer-Lombarte, A., Chen, S.-T., Malliaras, G.G., Barone, D.G., 2021. Foreign body reaction to implanted biomaterials and its impact in nerve neuroprosthetics. Front. Bioeng. Biotechnol. 9.

Chan, L.J., Ascher, D.B., Yadav, R., Bulitta, J.B., Williams, C.C., Porter, C.J.H., Landersdorfer, C.B., Kaminskas, L.M., 2016. Conjugation of 10 kDa linear PEG onto trastuzumab fab′ is sufficient to significantly enhance lymphatic exposure while preserving in vitro biological activity. Mol. Pharm. 13, 1229–1241.

Cirelli, K.M., Carnathan, D.G., Nogal, B., Martin, J.T., Rodriguez, O.L., Upadhyay, A.A., Enemuo, C.A., Gebru, E.H., Choe, Y., Viviano, F., Nakao, C., Pauthner, M.G., Reiss, S., Cottrell, C.A., Smith, M.L., Bastidas, R., Gibson, W., Wolabaugh, A.N., Melo, M.B., Cossette, B., Kumar, V., Patel, N.B., Tokatlian, T., Menis, S., Kulp, D.W., Burton, D.R., Murrell, B., Schief, W.R., Bosinger, S.E., Ward, A.B., Watson, C.T., Silvestri, G., Irvine, D.J., Crotty, S., 2019. Slow Delivery immunization enhances HIV neutralizing antibody and germinal center responses via modulation of immunodominance. Cell 177, 1153–1171.e1128.

Cirelli, K.M., Crotty, S., 2017. Germinal center enhancement by extended antigen availability. Curr. Opin. Immunol. 47, 64–69.

De Rose, R., Kent, S.J., Ranasinghe, C., 2015. Chapter 12 - Prime-Boost Vaccination: Impact on the HIV-1 Vaccine Field. In: Singh, M., Salnikova, M. (Eds.), Novel Approaches and Strategies for Biologics, Vaccines and Cancer Therapies. Academic Press, San Diego, pp. 289–313.

DeMuth, P.C., Li, A.V., Abbink, P., Liu, J., Li, H., Stanley, K.A., Smith, K.M., Lavine, C.L., Seaman, M.S., Kramer, J.A., Miller, A.D., Abraham, W., Suh, H., Elkhader, J., Hammond, P.T., Barouch, D.H., Irvine, D.J., 2013. Vaccine delivery with microneedle skin patches in nonhuman primates. Nat. Biotechnol. 31, 1082–1085.

DeMuth, P.C., Min, Y., Irvine, D.J., Hammond, P.T., 2014. Implantable silk composite microneedles for programmable vaccine release kinetics and enhanced immunogenicity in transcutaneous immunization. Adv. Healthc. Mater. 3, 47–58.

Dhalluin, C., Ross, A., Huber, W., Gerber, P., Brugger, D., Gsell, B., Senn, H., 2005. Structural, Kinetic, and thermodynamic analysis of the binding of the 40 kDa PEG−interferon-α2a and its individual positional isomers to the extracellular domain of the receptor IFNAR2. Bioconjug. Chem. 16, 518–527.

Di Lorenzo, F., Seiffert, S., 2015. Nanostructural heterogeneity in polymer networks and gels. Polym. Chem. 6, 5515–5528.

Dingels, C., Schömer, M., Frey, H., 2011. Die vielen Gesichter des Poly(ethylenglykol)s. Chem. Unserer Zeit 45, 338–349.

Erickson, H.P., 2009. Size and shape of protein molecules at the nanometer level determined by sedimentation, gel filtration, and electron microscopy. Biological Procedures Online 11, 32.

Gale, E.C., Powell, A.E., Roth, G.A., Meany, E.L., Yan, J., Ou, B.S., Grosskopf, A.K., Adamska, J., Picece, V.C.T.M., d'Aquino, A.I., Pulendran, B., Kim, P.S., Appel, E.A., 2021. Hydrogel-based slow release of a receptor-binding domain subunit vaccine elicits neutralizing antibody responses against SARS-CoV-2. Adv. Mater. 33, 2104362.

Giovannini, G., Kunc, F., Piras, C.C., Stranik, O., Edwards, A.A., Hall, A.J., Gubala, V., 2017. Stabilizing silica nanoparticles in hydrogels: impact on storage and polydispersity. RSC Adv. 7, 19924–19933.

Gregoritza, M., Goepferich, A.M., Brandl, F.P., 2016a. Polyanions effectively prevent protein conjugation and activity loss during hydrogel cross-linking. J. Control. Release 238, 92–102.
Gregoritza, M., Messmann, V., Goepferich, A.M., Brandl, F.P., 2016b. Design of hydrogels for delayed antibody release utilizing hydrophobic association and Diels-Alder chemistry in tandem. J. Mater. Chem. B 4, 3398–3408.
Gregoritza, M., Messmann, V., Abstiens, K., Brandl, F.P., Goepferich, A.M., 2017. Controlled antibody release from degradable thermoresponsive hydrogels cross-linked by diels-alder chemistry. Biomacromolecules 18, 2410–2418.
Guarecuco, R., Lu, J., McHugh, K.J., Norman, J.J., Thapa, L.S., Lydon, E., Langer, R., Jaklenec, A., 2018. Immunogenicity of pulsatile-release PLGA microspheres for single-injection vaccination. Vaccine 36, 3161–3168.
Hammer, N., Brandl, F.P., Kirchhof, S., Messmann, V., Goepferich, A.M., 2015. Protein compatibility of selected cross-linking reactions for hydrogels. Macromol. Biosci. 15, 405–413.
Jiang, X., Zhao, H., Li, W., 2022. Microneedle-mediated transdermal delivery of drug-carrying nanoparticles. Front. Bioeng. Biotechnol. 10.
Kastantin, M., Langdon, B.B., Chang, E.L., Schwartz, D.K., 2011. Single-molecule resolution of interfacial fibrinogen behavior: effects of oligomer populations and surface chemistry. J. Am. Chem. Soc. 133, 4975–4983.
Kirchhof, S., Brandl, F.P., Hammer, N., Goepferich, A.M., 2013. Investigation of the Diels-Alder reaction as a cross-linking mechanism for degradable poly(ethylene glycol) based hydrogels. J. Mater. Chem. B 1, 4855–4864.
Kirchhof, S., Abrami, M., Messmann, V., Hammer, N., Goepferich, A.M., Grassi, M., Brandl, F.P., 2015a. Diels-alder hydrogels for controlled antibody release: correlation between mesh size and release rate. Mol. Pharm. 12, 3358–3368.
Kirchhof, S., Gregoritza, M., Messmann, V., Hammer, N., Goepferich, A.M., Brandl, F.P., 2015b. Diels-Alder hydrogels with enhanced stability: first step toward controlled release of bevacizumab. Eur. J. Pharm. Biopharm. 96, 217–225.
Kirchhof, S., Strasser, A., Wittmann, H.-J., Messmann, V., Hammer, N., Goepferich, A.M., Brandl, F.P., 2015c. New insights into the cross-linking and degradation mechanism of Diels-Alder hydrogels. J. Mater. Chem. B 3, 449–457.
Kozma, G.T., Shimizu, T., Ishida, T., Szebeni, J., 2020. Anti-PEG antibodies: Properties, formation, testing and role in adverse immune reactions to PEGylated nano-biopharmaceuticals. Adv. Drug Deliv. Rev. 154–155, 163–175.
Li, J., Mooney, D.J., 2016. Designing hydrogels for controlled drug delivery. Nat. Rev. Mater. 1.
Liu, X., Kouassi, K.G.W., Vanbever, R., Dumoulin, M., 2022. Impact of the PEG length and PEGylation site on the structural, thermodynamic, thermal, and proteolytic stability of mono-PEGylated alpha-1 antitrypsin. Protein Sci. 31, e4392.
Liu, Y., Xiao, L., Joo, K.-I., Hu, B., Fang, J., Wang, P., 2014. In situ modulation of dendritic cells by injectable thermosensitive hydrogels for cancer vaccines in mice. Biomacromolecules 15, 3836–3845.
Lofano, G., Mallett, C.P., Bertholet, S., O'Hagan, D.T., 2020. Technological approaches to streamline vaccination schedules, progressing towards single-dose vaccines. Npj Vaccines 5, 88.
Menon, I., Bagwe, P., Gomes, K.B., Bajaj, L., Gala, R., Uddin, M.N., D'Souza, M.J., Zughaier, S.M., 2021. Microneedles: A New Generation Vaccine Delivery System. Micromachines (Basel) 12.
Moon, J.J., Suh, H., Li, A.V., Ockenhouse, C.F., Yadava, A., Irvine, D.J., 2012. Enhancing humoral responses to a malaria antigen with nanoparticle vaccines that expand Tfh cells and promote germinal center induction. PNAS 109, 1080–1085.
Noh, H.J., Noh, Y.-W., Heo, M.B., Kim, E.-H., Park, S.-J., Kim, Y.-I., Choi, Y.K., Lim, Y.T., 2016. Injectable and pathogen-mimicking hydrogels for enhanced protective immunity against emerging and highly pathogenic influenza virus. Small 12, 6279–6288.
Nunes, D., Andrade, S., Ramalho, M.J., Loureiro, J.A., Pereira, M.C., 2022. Polymeric Nanoparticles-Loaded Hydrogels for Biomedical Applications: A Systematic Review on In Vivo Findings. Polymers (Basel) 14.
Palgen, J.-L., Feraoun, Y., Dzangué-Tchoupou, G., Joly, C., Martinon, F., Le Grand, R., Beignon, A.-S., 2021. Optimize prime/boost vaccine strategies: trained immunity as a new player in the game. Front. Immunol. 12.
Peterhoff, D., Thalhauser, S., Sobczak, J.M., Mohsen, M.O., Voigt, C., Seifert, N., Neckermann, P., Hauser, A., Ding, S., Sattentau, Q., Bachmann, M.F., Breunig, M., Wagner, R., 2021a. Augmenting the immune response against a stabilized HIV-1 clade C envelope trimer by silica nanoparticle delivery. Vaccines (basel) 9, 642.
Peterhoff, D., Thalhauser, S., Sobczak, J.M., Mohsen, M.O., Voigt, C., Seifert, N., Neckermann, P., Hauser, A., Ding, S., Sattentau, Q., Bachmann, M.F., Breunig, M., Wagner, R., 2021b. Augmenting the immune response against a stabilized HIV-1 clade C envelope trimer by silica nanoparticle delivery. Vaccines (basel) 9.
Peterhoff, D., Thalhauser, S., Neckermann, P., Barbey, C., Straub, K., Nazet, J., Merkl, R., Laengst, G., Breunig, M., Wagner, R., 2022. Multivalent display of engineered HIV-1 envelope trimers on silica nanoparticles for targeting and in vitro activation of germline VRC01 B cells. Eur. J. Pharm. Biopharm. 181, 88–101.
Peterhoff, D., Wagner, R., 2017. Guiding the long way to broad HIV neutralization. Curr. Opin. HIV AIDS 12, 257–264.
Plesner, B., Fee, C.J., Westh, P., Nielsen, A.D., 2011. Effects of PEG size on structure, function and stability of PEGylated BSA. Eur. J. Pharm. Biopharm. 79, 399–405.
Roth, G.A., Gale, E.C., Alcántara-Hernández, M., Luo, W., Axpe, E., Verma, R., Yin, Q., Yu, A.C., Lopez Hernandez, H., Maikawa, C.L., Smith, A.A.A., Davis, M.M., Pulendran, B., Idoyaga, J., Appel, E.A., 2020. Injectable hydrogels for sustained codelivery of subunit vaccines enhance humoral immunity. ACS Cent. Sci. 6, 1800–1812.
Roth, G.A., Picece, V.C.T.M., Ou, B.S., Luo, W., Pulendran, B., Appel, E.A., 2022. Designing spatial and temporal control of vaccine responses. Nat. Rev. Mater. 7, 174–195.
Santos, J.H.P.M., Torres-Obreque, K.M., Meneguetti, G.P., Amaro, B.P., Rangel-Yagui, C. O., 2018. Protein PEGylation for the design of biobetters: from reaction to purification processes. Brazilian. J. Pharm. Sci. 54.
Schweizer, D., Vostiar, I., Heier, A., Serno, T., Schoenhammer, K., Jahn, M., Jones, S., Piequet, A., Beerli, C., Gram, H., Goepferich, A., 2013. Pharmacokinetics, biocompatibility and bioavailability of a controlled release monoclonal antibody formulation. J. Control. Release 172, 975–982.
Sekiya, T., Yamagishi, J., Gray, J.H.V., Whitney, P.G., Martinelli, A., Zeng, W., Wong, C. Y., Sugimoto, C., Jackson, D.C., Chua, B.Y., 2017. PEGylation of a TLR2-agonist-based vaccine delivery system improves antigen trafficking and the magnitude of ensuing antibody and CD8+ T cell responses. Biomaterials 137, 61–72.
Selis, F., Focà, G., Sandomenico, A., Marra, C., Di Mauro, C., Saccani Jotti, G., Scaramuzza, S., Politano, A., Sanna, R., Ruvo, M., Tonon, G., 2016. Pegylated trastuzumab fragments acquire an increased in vivo stability but show a largely reduced affinity for the target antigen. Int. J. Mol. Sci. 17, 491.
Slobbe, L., Medlicott, N., Lockhart, E., Davies, N., Tucker, I., Razzak, M., Buchan, G., 2003. A prolonged immune response to antigen delivered in poly (ϵ-caprolactone) microparticles. Immunol. Cell Biol. 81, 185–191.
Sun, S., Cui, Y., Yuan, B., Dou, M., Wang, G., Xu, H., Wang, J., Yin, W., Wu, D., Peng, C., 2023. Drug delivery systems based on polyethylene glycol hydrogels for enhanced bone regeneration. Front. Bioeng. Biotechnol. 11, 1117647.
Swartzlander, M.D., Barnes, C.A., Blakney, A.K., Kaar, J.L., Kyriakides, T.R., Bryant, S.J., 2015. Linking the foreign body response and protein adsorption to PEG-based hydrogels using proteomics. Biomaterials 41, 26–36.
Tam, H.H., Melo, M.B., Kang, M., Pelet, J.M., Ruda, V.M., Foley, M.H., Hu, J.K., Kumari, S., Crampton, J., Baldeon, A.D., Sanders, R.W., Moore, J.P., Crotty, S., Langer, R., Anderson, D.G., Chakraborty, A.K., Irvine, D.J., 2016. Sustained antigen availability during germinal center initiation enhances antibody responses to vaccination. P Natl Acad Sci USA 113 (E6639-E6648).
Thalhauser, S., Breunig, M., 2020. Considerations for efficient surface functionalization of nanoparticles with a high molecular weight protein as targeting ligand. Eur. J. Pharm. Sci. 155, 105520.
Thalhauser, S., Peterhoff, D., Wagner, R., Breunig, M., 2020a. Critical design criteria for engineering a nanoparticulate HIV-1 vaccine. J. Control. Release 317, 322–335.
Thalhauser, S., Peterhoff, D., Wagner, R., Breunig, M., 2020b. Presentation of HIV-1 envelope trimers on the surface of silica nanoparticles. J. Pharm. Sci. 109, 911–921.
Thalhauser, S., Peterhoff, D., Wagner, R., Breunig, M., 2020c. Silica particles incorporated into PLGA-based in situ-forming implants exploit the dual advantage of sustained release and particulate delivery. Eur. J. Pharm. Biopharm. 156, 1–10.
Victora, G.D., Nussenzweig, M.C., 2022. Germinal centers. Annu. Rev. Immunol. 40, 413–442.
Wagner, R., Hildt, E., 2019. Zusammensetzung und wirkmechanismen von adjuvanzien in zugelassenen viralen impfstoffen. Bundesgesundheitsbl. Gesundheitsforsch. Gesundheitsschutz 62, 462–471.
Wang, Y., Zhang, S., Benoit, D.S.W., 2018. Degradable poly(ethylene glycol) (PEG)-based hydrogels for spatiotemporal control of siRNA/nanoparticle delivery. J. Control. Release 287, 58–66.
Watermann, A., Brieger, J., 2017. Mesoporous silica nanoparticles as drug delivery vehicles in cancer. Nanomaterials 7, 189.
Yuan, W., Craig, S., Yang, X., Sodroski, J., 2005. Inter-subunit disulfide bonds in soluble HIV-1 envelope glycoprotein trimers. Virology 332, 369–383.
Ziegler, C.E., Graf, M., Nagaoka, M., Lehr, H., Goepferich, A.M., 2021. In situ forming iEDDA Hydrogels with tunable gelation time release high-molecular weight proteins in a controlled manner over an extended time. Biomacromolecules 22, 3223–3236.
Ziegler, C.E., Graf, M., Nagaoka, M., Goepferich, A.M., 2022. Investigation of the impact of hydrolytically cleavable groups on the stability of poly(ethylene glycol) based hydrogels cross-linked via the inverse electron demand diels-alder (iEDDA) reaction. Macromol. Biosci. 22, 2200226.